Published in final edited form as:
Free Radic Biol Med. 2012 September 1; 53(5): 1111–1122. doi:10.1016/j.freeradbiomed.2012.06.042.

Deficiency of αB crystallin augments ER stress induced apoptosis by enhancing mitochondrial dysfunction

Guorui Dou[a,b], **Parameswaran G Sreekumar**[a], **Christine Spee**[a,c], **Shikun He**[a,c,d], **Stephen J Ryan**[a,c], **Ram Kannan**[a,c], and **David R Hinton**[a,c,d,*]

[a]Arnold and Beckman Macular Research Center, Doheny Eye Institute, 1355 San Pablo St, Los Angeles, CA 90033, USA

[b]Department of Ophthalmology, Xijing Hospital, Fourth Military Medical University, Xi'an, China

[c]Department of Ophthalmology, Keck School of Medicine of the University of Southern California, Los Angeles, CA, 90033, USA

[d]Department of Pathology, Keck School of Medicine of the University of Southern California, Los Angeles, CA, 90033, USA

Abstract

Endoplasmic reticulum (ER) stress is linked to several pathological conditions including age-related macular degeneration. Excessive ER stress initiates cell death cascades which are mediated, in part, through mitochondrial dysfunction. Here, we identify αB crystallin as an important regulator of ER stress-induced cell death. Retinal pigment epithelial (RPE) cells from αB crystallin (−/−) mice, and human RPE cells transfected with αB crystallin siRNA, are more vulnerable to ER stress induced by tunicamycin. ER stress-mediated cell death is associated with increased levels of reactive oxygen species, depletion of glutathione in mitochondria, decreased superoxide dismutase activity, increased release of cytochrome c and activation of caspases 3 and 4. The ER stress signaling inhibitors, salubrinal and 4-(2-aminoethyl) benzenesulfonyl fluoride, decrease mitochondrial damage and reduce RPE apoptosis induced by ER stress. Prolonged ER stress decreases levels of αB crystallin, thus exacerbating mitochondrial dysfunction. Overexpression of αB crystallin protects RPE cells from ER stress-induced apoptosis by attenuating increases in Bax, CHOP, mitochondrial permeability transition, and cleaved caspase 3. Thus, these data collectively demonstrate that αB crystallin provides critical protection of mitochondrial function during ER stress-induced RPE apoptosis.

Keywords

Retinal pigment epithelium (RPE); endoplasmic reticulum (ER) stress; mitochondria; αB crystallin; apoptosis

*Corresponding Author: David R Hinton MD, Department of Pathology, 2011 Zonal Avenue, HMR 209, Los Angeles, CA 90033, USA. Tel.: + 1 323 442 6617; Fax: + 1 323 442 6688. dhinton@usc.edu.

INTRODUCTION

Age-related macular degeneration (AMD), a progressive degenerative retinal disease, is the leading cause of blindness among the elderly in developed countries. Retinal pigment epithelium (RPE) cells offer essential nutritional and metabolic support for light sensitive photoreceptors, and are a major pathologic target in the early and late stages of AMD [1]. Multiple cellular mechanisms are involved in the dysfunction and death of RPE cells in AMD, including accumulation of toxic metabolites, oxidative stress and inflammation [1, 2]. Recent studies suggest that endoplasmic reticulum (ER) stress also participates in the pathogenesis of RPE dysfunction in retinal degenerative disorders including AMD [3, 4].

Accumulation of unfolded proteins in the ER lumen results in “ER stress” and initiates a complex cellular response known as the unfolded protein response (UPR) [5]. This response is mediated through three ER transmembrane receptors: PRK (RNA-dependent protein kinase)-like ER /pancreatic eukaryotic translation initiation factor 2 subunit (eIF2) kinase (PERK/PEK), activating transcription factor-6 (ATF6), and the inositol-requiring enzyme 1(IRE1). Once UPR is triggered, cells first establish adaptive responses such as induction of ER chaperone GRP78 or global inhibition of protein synthesis. However, if this transcriptional program fails to reestablish ER homeostasis, signaling switches to a pro-apoptotic pathway [6].

The specific mechanisms involved in ER stress-induced apoptosis remain to be fully elucidated. The available evidence suggests that transcriptional induction of CHOP is critical in ER stress induced apoptosis [7]. Overexpression of CHOP can lead to cell cycle arrest and apoptosis, while CHOP $^{(-/-)}$ cells attenuated apoptosis in response to ER stress [7]. Activation of caspase cascades also occurs in ER stress. In rodents, earlier studies proposed that caspase 12 played a role in ER stress-induced apoptosis [6, 8], even though deletion of caspase 12 provides only partial protection against cell death [9]. However, a caspase 12-like protein in human cells contains a polymorphism that results in a truncated non functional protein [10]. Thus, recent studies have focused attention on caspase 4, which has been proposed to fulfill the function of caspase 12 in humans [11]. Caspase-dependent pathways of ER stress-induced apoptosis that are independent of caspase 4/12 have also been identified [12].

Mitochondria are recognized as the central regulator of apoptotic cell death and ER-mitochondrial crosstalk may mediate stress signals between these compartments [13]. Indeed, mitochondrial changes including loss of mitochondrial membrane potential (MPT), release of cytochrome c, and activation of caspase 9 and caspase 3 have been observed in ER stress [14]. A link between ER stress and reactive oxygen species (ROS), decrease in glutathione (GSH) and increase in calcium influx in the mitochondria has also been shown [15-17]. It has also been reported that CHOP, the ER stress induced transcription factor, not only down regulates Bcl-2 expression but also leads to translocation of Bax from cytosol to mitochondria [7, 18, 19]. The activation and mitochondrial localization of Bax [20, 21] and Apaf 1 (Apoptotic Protease-Activating Factor 1), which is required in post-mitochondrial apoptotic cascades, have been identified to contribute to mitochondrial impairment in ER stress induced apoptosis [22]. Thus, mitochondria are clearly linked to the development of ER stress-induced apoptosis.

Recently, the small heat shock protein αB crystallin has been identified as an important regulator of mitochondrial apoptosis; it inhibits oxidant-induced apoptosis in RPE and progression of retinal degeneration in animal models [23, 24, 25]. Expression of αB crystallin has also been linked to AMD, where its increased expression has been suggested to be a biomarker for the disease [26]. Expression of αB crystallin in RPE and its secretion

from the apical surface of human polarized RPE mediates neuroprotection to adjacent cells [23]. αB crystallin has been localized to several intracellular compartments including the mitochondria [24] but, little is known about its effect on ER stress and mitochondrial dysfunction. In the present study, we evaluate the role of αB crystallin in ER stress-mediated apoptosis in RPE, and demonstrate that αB crystallin provides critical protection of mitochondrial function in this process.

MATERIALS AND METHODS

Chemicals and Materials

Tunicamycin (TM) and AEBSF were obtained from Sigma Aldrich (St. Louis, MO). Salubrinal was obtained from Santa Cruz Biotechnology (Santa Cruz, CA). Caspase 4 inhibitor was obtained from BioVision (Mountain View, CA).

The αB crystallin knockout mice on 129S6/SvEvTac background were obtained from the National Eye Institute (courtesy of Dr. Eric Wawrousek, PhD), while 129S6/SvEvTac control mice were purchased from Taconic Farms (Germantown, NY). Isolation, culture and characterization of primary cultured RPE from knockout mice were performed as described [24]. All animal studies were conducted with adherence to the Association for Research in Vision and Ophthalmology (ARVO**)**. Statement for the Use of Animals in Ophthalmic and Vision Research and protocols were approved by the USC Institutional Animal Care and Use Committee (IACUC) under protocol # 11135 (continuing review approved January 25, 2012).

Studies using cultured human RPE (hRPE) were approved by the Institutional Review Board of the University of Southern California under protocol #HS-947005 (continuing review approved April 25, 2012) and adhered to the Declaration of Helsinki. hRPE cells were isolated from fetal human eyes from donors with written consent and were obtained from Advanced Bioscience Resources Inc. (Alameda, CA). Five donors were used for experiments, and donor to donor variation had a negligible effect on the results. The hRPE cells were cultured to 80-90% confluence in Dulbecco's modified Eagle medium (DMEM, Fisher Scientific, Pittsburgh, PA, USA) with 10% fetal bovine serum (FBS, Gibco BRL, Gaithersburg, MD, USA). They were changed to serum free media for 24 h before TM or other treatment. Cells were fully confluent at the time of treatments. Second to fourth passage cells were used in all experiments.

Generation of αB crystallin overexpressing stable cell line

αB crystallin overexpressing stable ARPE-19 cell line (αB^{+}) and control cell line ($pcDNA3.1^{+}$) were established using pcDNA3.1 plasmid [25]. Full length human αB crystallin cDNA was PCR-amplified and the PCR products were cloned into a pcDNA3.1 mammalian expression vector bearing the neomycin-resistance gene. The expression levels of αB crystallin were determined by immunoblot.

siRNA transfection

Human αB crystallin siRNA and scrambled control siRNA duplexes were prepared as described [27]. Briefly, 10 nM sense primer 5′-CCA GGG AGU UCC ACA GGA AdTdT-3′ and corresponding antisense primer 5′-UUC CUG UGG AAC UCC CUG GdTdT-3′ for αB crystallin; sense primer 5′-UUC UCC GAA CGU GUC ACG UdTdT-3′ and antisense primer 5′-ACG UGA CAC GUU CGG AGA AdTdT-3′ for scrambled control, were mixed respectively in 50 μl of water with 5 μl annealing buffer (Ambion). Forty-eight hours after transfection, cells were exposed to 3 μg/ml TM for 24 h and then harvested or fixed for further analysis.

Apoptosis assays

DNA cleavage of RPE cells from αB crystallin (−/−) mice and wild type mice, and of hRPE cells and transfected hRPE cells was measured by TdT-mediated dUTP nick-end labeling (TUNEL; In Situ Cell Death Detection Kit, Roche). After TM treatment, floating and adherent cells were collected and the assay was performed following manufacturer's protocol. Cells were analyzed by flow cytometry (Epics XL Flow Cytometer , Beckman Coulter; Brea, CA) or confocal microscopy (LSM510, Carl Zeiss, Thornweed, NY). Further differentiation between apoptotic versus necrotic types of cell death was studied by Annexin V and propidium iodide (PI) staining (Annexin V-FITC Apoptosis Kit, BioVision Inc., Mountain View, CA). Annexin V+/PI- cells indicated early stage apoptosis.

Mitochondrial membrane permeability transition

To assess MPT, a cell permeable cationic dye (Mito Flow; Cell Technology, Mountain View, CA) was added for 30 min to hRPE cells or αB crystallin overexpressing ARPE-19 cells pretreated with TM (3μg/ml) for 24 h and then analyzed by flow cytometry. Ten thousand events were recorded in each analysis. In this assay, healthy cells retain the reagent, while apoptotic cells exhibit a lower fluorescence signal due to loss of the dye.

Isolation and fractionation of proteins

Cells were harvested after the specified experimental period and total cellular protein was extracted from the cells [24]. Mitochondrial and cytosolic proteins were isolated using a commercial Mitochondria/Cytosol Fractionation Kit following manufacturer's protocol (BioVision Inc., Mountain View, CA). To check the efficiency of homogenization, suspensions were observed under a microscope. A shiny ring around the cell indicated intact cells, and 35 strokes with a dounce homogenizer lysed 90% of the cells. The lysates were first spun for 10 min at 700xg to remove cellular debris and then at 10,000xg for 30 min to pellet the mitochondria. The resulting supernatant was saved as the cytosol portion while the mitochondrial pellet was lysed with a mitochondria specific buffer. Harvested samples were collected for further analysis.

Immunoblot analysis

Immunoblotting was performed using the following antibodies: rabbit and mouse anti-αB crystallin antibody (Stressgen; San Diego, CA and Abcam, Cambridge, MA); rabbit anti-active caspase 3 and rabbit anti-caspase 4 (Cell Signaling Technology, Danvers, MA); mouse anti-tubulin, rabbit anti-COXIV, rabbit anti-caspase 3 (pro-and active-form), rabbit anti-Bcl-2 and rabbit anti-Bax (Santa Cruz Biotechnology, Santa Cruz, CA); rabbit anti-peIF2 and rabbit anti-ATF6 (GeneTex, Irvine, CA); mouse anti-cytochrome c (Abcam, Cambridge, MA); rabbit anti-GRP78 and rabbit anti-CHOP (Sigma-Aldrich, St. Louis, MO). After incubation with the secondary antibody (Vector Laboratories, Burlingame, CA), protein bands were detected by chemiluminescence (Thermo Scientific, Rockford, IL). To verify equal loading of proteins, PVDF membranes were stripped and incubated with glyceraldehyde-3-phosphate dehydrogenase (GAPDH) antibody (Millipore, Temecula, CA).

Immunoprecipitation

Binding of αB crystallin to caspase 3 was assessed by immunoprecipitation using anti-αB crystallin (Stressgen) and anti-caspase 3 (Santa Cruz Biotechnology) antibodies. In brief, 100 μg of total cell lysate from αB crystallin overexpressing cells or control cells were incubated with mouse monoclonal anti-αB crystallin antibody overnight at 4°C. Immunoprecipitates were then incubated with 2 mg/ml protein G-Sepharose (Invitrogen, Carlsbad, CA) for 2 h at 4°C, followed by centrifugation at 2000 rpm for 10 min.

Immunoprecipitates were then subjected to immunoblotting with rabbit anti-caspase 3 antibody and immunoreactive bands detected as described above.

Real-time PCR analysis

Quantitative expression of αB crystallin mRNA was examined using real-time PCR (LightCycler 480; Roche, IN). Trizol (GIBCO BRL, Rockville, MD) was used to extract RNA. One μg of total RNA was added to oligo (dT) 15 primer and AMV reverse transcriptase (Promega, Madison, WI) for the reverse transcriptase reaction. PCR was performed using SYBR Green Master Mix and GAPDH served as the internal control. Human primers were designed using Primer Express software (Applied Biosystems, Foster City, CA) and purchased from Qiagen (Valencia, CA): αB crystallin 5′-TCC CCA GAG GAA CTC AAA GTT AAG-3′ (278-301) and 5′-GGC GCT CTT CAT GTT TCC A-3′ (327-347); GAPDH 5′-CCA CAT CGC TCA GAC ACC AT-3′ (85-104) and 5′-GGC AAC AAT ATC CAC TTT ACC AGA GT-3′ (150-169). Relative change in mRNA expression was calculated to obtain the ΔΔCT values. Four separate sets of RNA were isolated and examined, and each set was tested in duplicate. Results were reported as fold change over controls.

Confocal microscopy

hRPE cells were grown on chamber slides and exposed to TM. To visualize the mitochondria and ER, mitochondria tracker or ER tracker (Molecular Probes, Eugene, OR) was added to samples for 30 min, prior to fixation with 4% paraformaldehyde. Cells were permeabilized with 0.1% TritonX-100 for 15 min, and then blocked with goat serum (Invitrogen, Carlsbad, CA) for 15 min. Primary antibodies were added to cells for 2 h at room temperature prior to addition of Texas Red-conjugated or fluorescence-conjugated secondary antibody (Vector Laboratories, Burlingame, CA) for 30 min. Slides were examined using a confocal microscope (LSM510, Thornwood, NY).

GSH analysis and SOD activity

GSH-Glo™ Glutathione Assay (Promega, WI) was utilized to measure unbound GSH according to manufacturer's protocol. Briefly, after isolation of mitochondria and cytosolic fractions as described above, the pellet containing whole mitochondria was suspended in 100 μl PBS in a 96-well plate. Luciferin-NT and Glutathione S-Transferase were added to GSH-Glo™ Buffer to make GSH-Glo™Reagent, which was then added to the plate containing mitochondrial and cytosolic fractions. After 30-minute incubation, reconstituted Luciferin Detection Reagent was added to the plate. Following 15-minute incubation, the plate was read in a luminometer and results were expressed as percent of control.

Mitochondrial superoxide dismutase (MnSOD) activity was measured in 20 μg total protein from RPE cells after inhibiting the cytosolic Cu-Zn SOD with potassium cyanide using a commercial kit (Cayman Chemical, Ann Arbor, MI). SOD activity was expressed as percent of control [28].

ROS assay

Levels of cytosolic reactive oxygen species (ROS) were assessed by adding 5 μM 2′,7′-dichlorodihydrofluorescein diacetate (H2-DCFH-DA) (Molecular Probes) for 20-30 min. The cells were then incubated with Mitotracker (Invitrogen, Carlsbad, CA) at a final concentration of 500 nM for 30 min to determine the compartmentalized distribution of ROS in mitochondria; cells were imaged with a confocal microscope.

MitoSOX assay

Mitochondrial superoxide production was measured by using MitoSOX Red Kit (Invitrogen, Carlsbad, CA) as described previously [29]. All experiments were performed in CO_2 incubator at 37 °C. For confocal microscopy, MitoSOX was added at 5 μM in the medium after treatment for 20 min and cells were washed before imaging. For flow cytometry measurement, cells were trypsinized for 2 min after 20 min MitoSOX loading and 10,000 cells were evaluated per condition.

Caspase 3 substrate cleavage assay

Caspase 3 was measured using colorimetric assay kits (BioVision). Cells were collected and washed with ice-cold PBS and then resuspended in chilled lysis buffer for 20 min on ice. The supernatant was collected by centrifugation at 10,000 g for 5 min. Cell lysates (20 μg protein) were incubated with 0.5 mM Ac-DEVD-*p*NA (caspase 3) in a final volume of 100 μl. The release of the chromogenic compound *p*NA from the incubated lysates was measured by absorbance at 405 nm using a micro plate reader (Bio-Rad, Irvine, CA).

Statistical analysis

All experiments were performed at least three times. Statistical analyses were performed using Tukey's or Dunnett's tests for multiple comparisons. All of the tests were two-sided and $p<0.05$ was accepted as significant. The statistic and graphic software GraphPad Prism (Version 5, GraphPad Software, Inc., La Jolla, CA) was used for all statistical and graphic analysis.

RESULTS

Pilot studies were conducted with several pro-apoptotic agents that specifically induce ER stress. They included tunicamycin (an inhibitor of N-linked glycosylation), brefeldin (BFA, an inhibitor of ER-Golgi transport) and thapsigargin (TG, an inhibitor of ER Ca^{2+} uptake). These studies showed that in the absence of αB crystallin, all three ER stressors induced cell death when compared to wild type RPE cells (data not shown). We chose TM to induce ER stress in RPE cells since TM has been used in some *in vivo* ocular studies [30, 31].

ER stress induces GRP78, CHOP, caspase 4 and caspase 3 activation

In preliminary experiments, hRPE cells were exposed to 100 ng/ml-20 μg/ml TM for specified time periods namely, 30 min, 1h, 2h, 6h, 12h, 24h and 48h. 0.1-1% DMSO vehicle was used for control cells. Cell viability as determined by trypan blue exclusion showed that higher TM concentrations (>10 μg/ml) and longer treatment (>24h) resulted in significant loss of viability of hRPE cells. Thus, for subsequent experiments we induced ER stress with 3 and 10 μg/ml TM for 6 and 24h; at these concentrations and time points, viability remained at 65% or greater (Supplementary Figure 1). As shown in Fig.1A, expression of ER stress marker proteins such as GRP78 and CHOP was significantly elevated with TM treatment after 6, 12 or 24 h of incubation.

Immunoblot analysis and immunofluorescent staining showed proteolytic activation of caspase 4 in a time dependent manner upon exposure to 3 μg/ml TM (Fig.1B, C). Further, double labeling of cleaved caspase 4 with ER tracker confirmed localization of this caspase to the ER (Fig. 1B). In addition, TM treatment (3μg/ml 24h) resulted in accumulation of active caspase 3 in the perinuclear region (Fig.2A). Immunoblot analysis revealed that activation of caspase 3 cleavage was only modest with 3 μg/ml TM for 6h, but higher dosage (10 μg/ml) or longer treatment (3 μg/ml 24h) resulted in a significant induction (Fig. 2B). These results show that caspase 3 and caspase 4 are activated by ER stress in hRPE cells.

ER stress leads to ROS formation, depletion of GSH and decreased MnSOD activity in hRPE cells

To determine whether ROS contribute to apoptotic cell death under ER stress, generation of ROS was measured in cells with or without TM treatment. In hRPE cells treated with 3 μg/ml TM, ROS formation was seen at 6h and 24h, and the ROS-associated DCF fluorescence partially co- localized with mitochondria (Mitotracker) (Fig.3A), indicating that ROS generated by ER stressor can cause oxidative damage to mitochondria and potentially perturb mitochondrial homeostasis. In addition, MitoSOX was used to specifically quantify the formation of mitochondrial ROS. MitoSOX Red is a fluorogenic dye recently developed and validated for highly selective detection of superoxide in the mitochondria of live cells [30]. Confocal microscopic imaging demonstrated a prominent increase in mitochondrial fluorescence of MitoSOX in hRPE cells treated with 3 μg/ml TM at 6h and 24h (Fig. 3B). Consistent with this finding, MitoSOX analysis by flow cytometry revealed a significant increase in mean intensity of fluorescence in hRPE treated with TM for 24 h (Fig.3C). The effect of TM on MnSOD activity was also determined. As shown in Fig. 3D, MnSOD activity decreased significantly ($p<0.05$ vs untreated controls) in cells treated with 3 μg/ml TM for 6 h and 24 h. The measured activity represents MnSOD activity in mitochondria since Cu-Zn SOD present in the lysate was inhibited prior to analysis [28]. ER stress may promote oxidative stress by disturbance of redox status through depletion of GSH [32]. In TM-treated hRPE cells, cytosolic GSH was significantly reduced at 24 h, while mitochondrial GSH was significantly decreased at both 6 and 24h (Fig.3E). These observations suggest that disturbance of redox status at the mitochondrial level participates in the process of ER stress-mediated cell damage in hRPE cells.

Upregulation of Bcl-2 and Bax under ER stress in hRPE

Bcl-2 family proteins has been suggested to regulate the homeostatic function of mitochondria in ER stress-initiated apoptosis [33]. In the present study, we found that TM increased expression of pro-apoptotic Bax and anti-apoptotic Bcl-2 protein in hRPE cells (Fig.4). The Bcl-2/Bax ratio showed a significant increase with 10μg/ml TM for 6h. Since the ratio of Bcl-2 to Bax is generally considered to determine susceptibility to cell death following an apoptotic stimulus, these observations suggest an early protective response of hRPE cells to apoptotic stimuli at 6 h that is lost by 24 h of incubation.

Release of cytochrome c from mitochondria in hRPE cells under ER stress

Release of cytochrome c is a critical apoptotic event at the level of the mitochondria and can in turn promote programmed death by activating apoptotic cascades. We therefore studied whether ER stress could lead to cytochrome c release from mitochondria. As shown in Fig. 5A, control cells retained cytochrome c in mitochondria. After 10 μg/ml TM treatment for 6h or 3 μg/ml TM treatment for 24h, cytochrome c was released from mitochondria, resulting in increased cytosolic staining. Consistent with the confocal imaging, immunoblot analysis of mitochondrial and cytosolic cytochrome c further revealed that cytosolic cytochrome c increased approximately 2.5 fold in TM treated cells compared to the control (Fig.5B).

ER stress inhibitors attenuate TM-induced mitochondrial dysfunction and cell death

Small molecules have been identified with inhibitory effects on ER stress *in vitro* and *in vivo*. Salubrinal is found to protect cells from TM induced apoptosis by selectively activating the peIF2α branch of the unfolded protein response [34]. 4-(2-aminoethyl) benzenesulfonyl fluoride (AEBSF), a serine protease inhibitor, is reported to inhibit the ER stress induced proteolysis of ATF6, resulting in inhibition of transcriptional induction of ATF6-target genes by ER stress [35].

To investigate whether Salubrinal and AEBSF have the ability to prevent mitochondrial dysfunction and cell death induced by TM in hRPE cells, we treated hRPE cells with 25 μM Salubrinal and 0-300 μM AEBSF for 2 h prior to TM treatment. As expected, the level of p-elF2α was increased by 25 μM Salubrinal in TM (3μg/ml 24h) treated hRPE cells and 300 μM AEBSF inhibited the TM-induced nuclear translocation and proteolysis of ATF6 (Supplementary Fig2.A,B,C). Pretreatment with Salubrinal and AEBSF significantly inhibited MPT that was induced by TM (Fig 6A). In addition, TM-induced hRPE cell death as was significantly reduced by pretreatment with 25 μM Salubrinal and 300 μM AEBSF (Fig 6B).

Lack of αB crystallin expression augments the vulnerability of RPE cells to ER stress-induced cell death

To determine whether deficiency of αB crystallin during ER stress renders RPE cells more vulnerable to lethal insult, αB crystallin (−/−) RPE and hRPE transfected with αB crystallin siRNA were evaluated for their sensitivity to TM. RPE cells isolated from αB crystallin (−/−) and wild-type mice were treated with 50 ng/ml or 100 ng/ml TM for 24 h. Adherent and detached cells were harvested and stained by TUNEL and then analyzed by flow cytometry. αB crystallin (−/−) RPE cells showed a dose dependent increase in apoptosis after TM treatment compared to wild type cells (left panel in Fig.7A). Following the induction of ER stress, we also observed an increase in the proteolytic cleavage of caspase 3 in TM treated RPE cultured from αB crystallin (−/−) animals compared with wild type controls (right panel in Fig.7A). hRPE cells transfected with αB crystallin siRNA showed a 70% decrease in the basal level of αB crystallin protein expression, compared with non-silenced and scrambled siRNA control cells, while the basal level of GRP78 did not change (Fig.7B). αB crystallin siRNA transfected cells showed increased sensitivity to TM-induced apoptosis at both 6 and 24 h (Fig.7C). Analysis of cell death by Annexin V and PI assay in siRNA transfected cells with TM treatment for 24h showed that >90% of the dead cells were AnnexinV positive/PI negative, confirming that cell death from TM treatment in siRNA transfected cells was predominantly by apoptosis (Fig.7D). It is noteworthy that under these conditions, basal and ER stress-induced expression of GRP78 were unaffected by knockout or knockdown of αB crystallin (data not shown). Together, these results indicate that αB crystallin has a significant effect on cell death induced by ER stress, which may be independent of GRP78.

Overexpression of αB crystallin protects RPE cells against ER stress-induced cell death by inhibiting caspase 3 activation and increased MPT

To determine the effects of elevated αB crystallin protein levels on ER stress, we developed a stable cell line overexpressing αB crystallin in ARPE-19 cells. The level of αB crystallin protein in stably transfected cells was 4-8 fold higher than the transfected control cells (ARPE-19 pcDNA$^+$) (upper panel in Fig.8A). Upon exposure to 3μg/ml TM for 6h and 24h, ARPE-19αB$^+$ cells showed reduction in TM-induced cell death by 50% (lower panel in Fig. 8A). Caspase 3 activation induced by TM was significantly inhibited in αB crystallin stably transfected cells compared with control cells (upper panel in Fig.8B). To explore how αB crystallin repressed caspase 3 activity, immunoprecipitation assays were performed. In anti-αB crystallin immunoprecipitates from cell lysates of ARPE-19αB$^+$ cells and control cells, procaspase 3 expression was much more abundant in ARPE-19αB$^+$ cell immunoprecipitates than in ARPE-19 pcDNA$^+$ cell immunoprecipitates (lower panel in Fig.8B), indicating one of the mechanisms by which αB crystallin regulates caspase 3 activation is through binding of αB crystallin to procaspase 3. To explain the possibility that the protective action of αB crystallin is mediated by changes in the level of the unfolded protein response, we analyzed the levels of GRP78 in ARPE-19αB$^+$ cells and controls treated by TM. Basal and up regulated levels of GRP78 in ARPE-19αB$^+$ cells were comparable to those in control cells,

indicating that αB crystallin overexpression alone does not influence this ER stress specific chaperone (Fig.8C). However, we observed that ER stress-induced CHOP expression was suppressed in ARPE-19αB$^+$ cells (Fig.8C). Thus, the αB crystallin mediated RPE protective effect seems to be independent of GRP78, but cell death may be directly or indirectly influenced by CHOP.

Apoptosis triggered by ER stress may involve mitochondrial alterations that include Bax translocation, and induction of MPT [19, 36]; αB crystallin may interact with Bcl-2 family members to regulate these cell death cascades [37-40]. Therefore, we evaluated MPT in ARPE 19 cells following exposure to 3μg/ml TM for 24 h. TM induced MPT in ARPE-19 cells and this effect was significantly attenuated in ARPE-19αB$^+$ cells (Fig.8D,E). This demonstrates that αB crystallin could also protect mitochondrial membrane permeability during ER stress.

ER stress downregulates expression of αB crystallin in hRPE cells

Based on the above observations that lack of αB crystallin enhanced the sensitivity of RPE cells to ER stress-induced apoptosis while overexpression of αB crystallin protected hRPE cells, we hypothesized that expression of αB crystallin might be regulated during prolonged ER stress. Indeed, αB crystallin expression at both the protein and mRNA level showed a small but not significant increase upon low dose TM treatment. In contrast, with high dosage and longer treatment, there was a significant decrease in αB crystallin protein and mRNA level (Fig. 9A and B). The decrease in αB crystallin was observed in mitochondria as evidenced by co-localization with Mitotracker (Supplementary Fig.3). In addition, when ER stress was mitigated by ER stress inhibitors Salubrinal and AEBSF through inhibition of PERK and ATF6 signaling pathways respectively, the decrease in αB crystallin expression was attenuated (Fig 9C). Thus in the presence of severe ER stress, deficiency of αB crystallin further incapacitates the RPE to defend against ER stress. Our finding that Salubrinal and AEBSF also reduced TM-induced RPE mitochondrial dysfunction and apoptosis indicates that preventing the loss of αB crystallin could be one of the mechanisms of their protective effect.

DISCUSSION

Our data show that ER stress activates caspase 4 and the cell death that results also involves several mitochondrial apoptotic events. Further, we also show that deficiency of αB crystallin renders RPE susceptible to ER stress-induced cell death while overexpression results in protection. We have recently reported that deficiency of αB crystallin protects against development of choroidal neovascularization (CNV) in mice [27]. Here we are show that αB crystallin protects RPE cells from both oxidative and ER stress-induced apoptosis. The resulting apparent paradox is that while high levels of αB crystallin would be protective for stressed RPE, low levels of αB crystallin would be protective against pathologic angiogenesis. However, αB crystallin has many other effects that are also anti-angiogenic, especially its strongly anti-inflammatory effects [41]; therefore αB crystallin deficiency may protect against CNV, while increased αB crystallin expression could also inhibit CNV based on its anti-inflammatory effect. Further experimentation is warranted to evaluate this apparent paradox.

Activators of ER stress-induced apoptosis have been described in many retinal cell types including photoreceptors, ganglion cells, and endothelial cells [30, 42, 43]. In this study, we characterized ER stress by the upregulation of ER stress markers GRP78 and CHOP when RPE cells were treated with TM. The mechanism of ER stress-induced apoptosis is mediated through ER resident caspase 4 [14, 37]. Caspase 4 has a CARD domain through which caspase 9 and Apaf-1 interact and form an apoptosome complex [44].The caspase 4 inhibitor

Z-LEVD-fmk or knockdown of caspase 4 effectively inhibits ER stress-induced apoptosis in many cell types [45]. Accordingly, in the present study we observed that TM caused early activation of caspase 4 and inhibition of caspase 4 activity attenuated ER stress induced RPE cell death, an observation in corroboration with a recent study in RPE cells [37].

Unfolded protein response (UPR) is initiated with three ER stress inhibitors; IRE-1, ATF6 and PERK-elF2α known to result from upregulation of molecular chaperones which prevent further accumulation of unfolded proteins [35]. We found that salubrinal (inhibitor of PERK pathway) and AEBSF (inhibitor of ATF6 pathway) decreased the apoptotic cells and inhibited the increase in MPT from TM treatment indicating that PERK-elF2α and ATF6 might be involved in ER stress induced mitochondrial dysfunction in RPE cells. The specific mechanisms how each of these signaling pathway influences the mitochondrial function need to be further clarified.

Apart from ER specific apoptotic pathway, the capacity of ER stress to induce cell death through a series of events at the mitochondrial level has been suggested [36]. Release of cytochrome c from mitochondria during ER stress-induced apoptosis is mediated by MPT [20, 46, 47]. Consistent with this, release of cytochrome c in hRPE cells under ER stress was accompanied by an increase in MPT in this study.

The redox status of a cell can also influence mitochondrial function. GSH can potentially confer protection against apoptotic insults to mitochondria [48]. Changes in free GSH in cytosol and mitochondria under ER stress could partly offset mitochondrial dysfunction [16]. Moreover, ER stress-induced ROS production may also be initiated by ER, pushing mitochondrial ROS above the cell survival threshold, leading to cell death [49]. It is likely that mitochondrial ROS can impair ER function via enhancement of ER stress and UPR [50]. Direct or indirect ROS action appears to largely mediate cytochrome c release from mitochondria, which consequently triggers caspase activation [51]. We found in TM treated hRPE cells, ER stress markedly decreased mitochondrial GSH and MnSOD activity. This raises the possibility that under ER stress, supplementation of mitochondrial GSH or overexpression of MnSOD can offer protection against oxidative damage that could compromise the vital mitochondrial function.

αB crystallin has been shown to have antiapoptotic properties in RPE cells [25, 39]. In AMD, αB crystallin is expressed in RPE in association with subretinal drusen deposits and it is more prominently expressed in the late stage of the disease [26]. Deficiency of αB crystallin sensitizes RPE cells and other cells to external stress [24, 52, 53]. Here, we report that prolonged ER stress downregulates αB crystallin and pre-treatment with ER stress inhibitors restored αB crystallin, suggesting its protective role in TM-treated RPE. In support, ER stress was significantly elevated in calcineurin overexpressing conditional transgenic mice, however, apoptosis was inhibited and proteomic studies identified increased levels of αB crystallin as a potential mediator of this protective effect [54]. Selective disruption of UPR pathways (IRE1, XBP-1, ATF6) or knockdown of αB crystallin significantly increased vascular endothelial growth factor (VEGF) proteolytic degradation showing a crucial role of UPR/ αB crystallin in maintaining endothelial VEGF [55].

The protective mechanism of αB crystallin has been linked to the interplay with Bcl-2 family proteins [38, 39]. It is increasingly evident that Bcl-2 family members, have an essential role in apoptotic pathways initiated by ER stress. Mitochondrial Bax is required for ER initiated apoptosis [20]. Up-regulation of mitochondrial Bcl-2 has been shown to prevent Bax activation and, as a result, preserve the integrity of mitochondria and maintain cytochrome c in the organelles [56]. The re-localization of Bcl-2 and Bax to mitochondria and increased Bcl-2/Bax ratio in hRPE cells under ER stress suggest an early protective

response of hRPE cells to apoptotic stimuli by enhanced expression of Bcl-2 to counteract the increase in pro-apoptotic protein Bax. In this context, the biphasic nature of Bax translocation to mitochondria has to be recognized [57]. However, decreased αB crystallin under ER stress may attenuate protective capacity of Bcl-2, which results in RPE apoptosis. Notably, we found overexpression of αB crystallin in RPE cells could depress the up-regulation of Bax induced by ER stress, suggesting a possible mechanism of αB crystallin to defend ER stress. Besides, it is possible that αB crystallin can modulate other proteins to regulate Bax. CHOP can regulate several Bcl-2 family proteins including Bax [58] and accordingly we also found that the induction of CHOP is greatly abrogated by αB crystallin overexpression.

The opening of MPT pores is a regulator in the crosstalk between ER and mitochondria [17, 46]. Loss of cytochrome c, leads the electron transport chain to produce more free radicals [59]. Additionally, increasing permeability of mitochondria enables GSH to exit mitochondria, reducing the organelles' ability to neutralize superoxides and ROS. The mitochondria thus play an important role to amplify the apoptotic signaling from ER through MPT. Recently, αB crystallin has been reported to regulate the MPT pore opening [24, 60]. Our data show for the first time that overexpression of αB crystallin could restore MPT affected by ER stress, suggesting that αB crystallin protects RPE cells against ER stress by restoring mitochondrial function.

αB Crystallin exerts anti apoptotic effect via the disruption of proteolytic activation of caspase 3 [61-62]. Furthermore, in astrocytes αB crystallin can bind to procaspase 3 to inhibit activation and confer protection against oxidative stress [63]. We report in this study that overexpression of αB crystallin in RPE cells can result in increased binding to procaspase 3, and the activation of caspase 3 is greatly repressed in αB crystallin overexpressing RPE cells.

We also found that the induction of CHOP is greatly abrogated by αB crystallin overexpression. CHOP, which contains ER stress response element (ERSE) sequence, is a highly inducible gene in ER stress and can be activated by the proapoptotic proteins, p38-MAP kinase and JNK [5, 63]. In addition, mitochondrial ROS can positively control CHOP expression [64]. The exact mechanism of CHOP regulation by αB crystallin in RPE cells needs further investigation.

In conclusion, while the molecular mechanism involved in ER stress-mediated apoptosis is complex, our study points to the mitochondria-interconnected pathways playing a critical role in amplifying apoptotic signaling in RPE cells. Our study underlines the importance of combinational treatment approaches for disease like AMD that manifest hallmarks of ER stress and apoptosis. These approaches should target not only ER specific pathways, but also pathways involving mitochondrial function, and molecules like αB crystallin, are therefore potent candidates for such comprehensive treatment approaches [65].

Supplementary Material

Refer to Web version on PubMed Central for supplementary material.

Acknowledgments

We thank Jennifer Yaung, Ph D. for assistance in preliminary experiments and Eric A. Barron and Ernesto Barron for expert technical help.

Support: Supported in part by grant EY01545 (SJR, DRH) and by core grant EY03040; the Arnold and Mabel Beckman Foundation; an unrestricted grant to the Department of Ophthalmology from Research to Prevent Blindness Inc., New York, NY.

Abbreviations

ER	endoplasmic reticulum
AMD	age-related macular degeneration
RPE	retinal pigment epithelium
TM	tunicamycin
ROS	reactive oxygen species
GSH	glutathione
MPT	mitochondrial permeability transition
UPR	unfolded protein response
BFA	brefeldin
TG	thapsigargin

References

[1]. Zarbin MA, Rosenfeld PJ. Pathway-based therapies for age-related macular degeneration: an integrated survey of emerging treatment alternatives. Retina. 2010; 30:1350–1367. [PubMed: 20924259]

[2]. Bird AC. Therapeutic targets in age-related macular disease. J Clin Invest. 2010; 120:3033–3041. [PubMed: 20811159]

[3]. Mendes CS, Levet C, Chatelain G, Dourlen P, Fouillet A, Dichtel-Danjoy ML, Gambis A, Ryoo HD, Steller H, Mollereau B. ER stress protects from retinal degeneration. EMBO J. 2009; 28:1296–1307. [PubMed: 19339992]

[4]. He S, Yaung J, Kim YH, Barron E, Ryan SJ, Hinton DR. Endoplasmic reticulum stress induced by oxidative stress in retinal pigment epithelial cells. Graefes Arch Clin Exp Ophthalmol. 2008; 246:677–683. [PubMed: 18278507]

[5]. Xu C, Bailly-Maitre B, Reed JC. Endoplasmic reticulum stress: cell life and death decisions. J Clin Invest. 2005; 115:2656–2664. [PubMed: 16200199]

[6]. Kim I, Xu W, Reed JC. Cell death and endoplasmic reticulum stress: disease relevance and therapeutic opportunities. Nat Rev Drug Discov. 2008; 7:1013–1030. [PubMed: 19043451]

[7]. Oyadomari S, Mori M. Roles of CHOP/GADD153 in endoplasmic reticulum stress. Cell Death Differ. 2004; 11:381–389. [PubMed: 14685163]

[8]. Van de Craen M, Vandenabeele P, Declercq W, Van den Brande I, Van Loo G, Molemans F, Schotte P, Van Criekinge W, Beyaert R, Fiers W. Characterization of seven murine caspase family members. FEBS Lett. 1997; 403:61–69. [PubMed: 9038361]

[9]. Sanges D, Marigo V. Cross-talk between two apoptotic pathways activated by endoplasmic reticulum stress: differential contribution of caspase-12 and AIF. Apoptosis. 2006; 11:1629–1641. [PubMed: 16820963]

[10]. Saleh M, Vaillancourt JP, Graham RK, Huyck M, Srinivasula SM, Alnemri ES, Steinberg MH, Nolan V, Baldwin CT, Hotchkiss RS, Buchman TG, Zehnbauer BA, Hayden MR, Farrer LA, Roy S, Nicholson DW. Differential modulation of endotoxin responsiveness by human caspase-12 polymorphisms. Nature. 2004; 429:75–79. [PubMed: 15129283]

[11]. Hitomi J, Katayama T, Eguchi Y, Kudo T, Taniguchi M, Koyama Y, Manabe T, Yamagishi S, Bando Y, Imaizumi K, Tsujimoto Y, Tohyama M. Involvement of caspase-4 in endoplasmic reticulum stress-induced apoptosis and Abeta-induced cell death. J Cell Biol. 2004; 165:347–356. [PubMed: 15123740]

[12]. Obeng EA, Boise LH. Caspase-12 and caspase-4 are not required for caspase-dependent endoplasmic reticulum stress-induced apoptosis. J Biol Chem. 2005; 280:29578–29587. [PubMed: 15975932]

[13]. Ouyang YB, Xu LJ, Emery JF, Lee AS, Giffard RG. Overexpressing GRP78 influences Ca(2+) handling and function of mitochondria in astrocytes after ischemia-like stress. Mitochondrion. 2010 doi:10.1016/j.mito.2010.10.007;

[14]. Momoi T. Caspases involved in ER stress-mediated cell death. J Chem Neuroanat. 2004; 28:101–105. [PubMed: 15363495]

[15]. Lluis JM, Colell A, Garcia-Ruiz C, Kaplowitz N, Fernandez-Checa JC. Acetaldehyde impairs mitochondrial glutathione transport in HepG2 cells through endoplasmic reticulum stress. Gastroenterology. 2003; 124:708–724. [PubMed: 12612910]

[16]. Ikesugi K, Yamamoto R, Mulhern ML, Shinohara T. Role of the unfolded protein response (UPR) in cataract formation. Exp Eye Res. 2006; 83:508–516. [PubMed: 16643900]

[17]. Sharaf El Dein O, Gallerne C, Deniaud A, Brenner C, Lemaire C. Role of the permeability transition pore complex in lethal inter-organelle crosstalk. Front Biosci. 2009; 14:3465–3482. [PubMed: 19273287]

[18]. McCullough KD, Martindale JL, Klotz LO, Aw TY, Holbrook NJ. Gadd153 sensitizes cells to endoplasmic reticulum stress by down-regulating Bcl2 and perturbing the cellular redox state. Mol Cell Biol. 2001; 21:1249–1259. [PubMed: 11158311]

[19]. Gotoh T, Terada K, Oyadomari S, Mori M. hsp70-DnaJ chaperone pair prevents nitric oxide- and CHOP-induced apoptosis by inhibiting translocation of Bax to mitochondria. Cell Death Differ. 2004; 11:390–402. [PubMed: 14752510]

[20]. Zhang D, Armstrong JS. Bax and the mitochondrial permeability transition cooperate in the release of cytochrome c during endoplasmic reticulum-stress-induced apoptosis. Cell Death Differ. 2007; 14:703–715. [PubMed: 17170750]

[21]. Scorrano L, Oakes SA, Opferman JT, Cheng EH, Sorcinelli MD, Pozzan T, Korsmeyer SJ. BAX and BAK regulation of endoplasmic reticulum Ca2+: a control point for apoptosis. Science. 2003; 300:135–139. [PubMed: 12624178]

[22]. Smith MI, Deshmukh M. Endoplasmic reticulum stress-induced apoptosis requires bax for commitment and Apaf-1 for execution in primary neurons. Cell Death Differ. 2007; 14:1011–1019. [PubMed: 17218955]

[23]. Sreekumar PG, Kannan R, Kitamura M, Spee C, Barron E, Ryan SJ, Hinton DR. alphaB crystallin is apically secreted within exosomes by polarized human retinal pigment epithelium and provides neuroprotection to adjacent cells. PLoS One. 2010; 5:e12578. [PubMed: 20949024]

[24]. Yaung J, Jin M, Barron E, Spee C, Wawrousek EF, Kannan R, Hinton DR. alpha Crystallin distribution in retinal pigment epithelium and effect of gene knockouts on sensitivity to oxidative stress. Mol Vis. 2007; 13:566–577. [PubMed: 17438522]

[25]. Sreekumar PG, Spee C, Ryan SJ, Cole SP, Kannan R, Hinton DR. Mechanism of RPE Cell Death in Crystallin Deficient Mice: A Novel and Critical Role for MRP1-Mediated GSH Efflux. PLoS One. 2012; 3:e33420. [PubMed: 22442691]

[26]. De S, Rabin DM, Salero E, Lederman PL, Temple S, Stern JH. Human retinal pigment epithelium cell changes and expression of alphaB-crystallin: a biomarker for retinal pigment epithelium cell change in age-related macular degeneration. Arch Ophthalmol. 2007; 125:641–645. [PubMed: 17502503]

[27]. Kase S, He S, Sonoda S, Kitamura M, Spee C, Wawrousek E, Ryan SJ, Kannan R, Hinton DR. AlphaB crystallin regulation of angiogenesis by modulation of VEGF. Blood. 2009; 22:3398–3406. [PubMed: 20023214]

[28]. Kowluru RA, Kowluru V, Xiong Y, Ho YS. Overexpression of mitochondrial superoxide dismutase in mice protects the retina from diabetes-induced oxidative stress. Free Radic Biol Med. 2006; 41:1191–1196. [PubMed: 17015165]

[29]. Mukhopadhyay P, Rajesh M, Yoshihiro K, Hasko G, Pacher P. Simple quantitative detection of mitochondrial superoxide production in live cells. Biochem Biophys Res Commun. 2007; 358:203–208. [PubMed: 17475217]

[30]. Li J, Wang JJ, Yu Q, Wang M, Zhang SX. Endoplasmic reticulum stress is implicated in retinal inflammation and diabetic retinopathy. FEBS Lett. 2009; 583:1521–1527. [PubMed: 19364508]

[31]. Shimazawa M, Inokuchi Y, Ito Y, Murata H, Aihara M, Miura M, Araie M, Hara H. Involvement of ER stress in retinal cell death. Mol Vis. 2007; 13:578–587. [PubMed: 17438523]

[32]. Forman HJ, Zhang H, Rinna A. Glutathione: overview of its protective roles, measurement, and biosynthesis. Mol Aspects Med. 2009; 30:1–12. [PubMed: 18796312]

[33]. Hetz CA. ER stress signaling and the BCL-2 family of proteins: from adaptation to irreversible cellular damage. Antioxid Redox Signal. 2007; 9:2345–2355. [PubMed: 17854276]

[34]. Boyce M, Bryant KF, Jousse C, Long K, Harding HP, Scheuner D, Kaufman RJ, Ma D, Coen DM, Ron D, Yuan J. A selective inhibitor of eIF2alpha dephosphorylation protects cells from ER stress. Science. 2005; 307:935–939. [PubMed: 15705855]

[35]. Tabas I, Ron D. Integrating the mechanisms of apoptosis induced by endoplasmic reticulum stress. Nature Cell Biol. 2011; 13:184–190. [PubMed: 21364565]

[36]. Timmins JM, Ozcan L, Seimon TA, Li G, Malagelada C, Backs J, Backs T, Bassel-Duby R, Olson EN, Anderson ME, Tabas I. Calcium/calmodulin-dependent protein kinase II links ER stress with Fas and mitochondrial apoptosis pathways. J Clin Invest. 2009; 119:2925–2941. [PubMed: 19741297]

[37]. Bian ZM, Elner SG, Elner VM. Dual involvement of caspase 4 in inflammatory and ER stress-induced apoptotic responses in human retinal pigment epithelial cells. Invest Ophthalmol Vis Sci. 2009; 50:6006–6014. [PubMed: 19643964]

[38]. Mao YW, Xiang H, Wang J, Korsmeyer S, Reddan J, Li DW. Human bcl-2 gene attenuates the ability of rabbit lens epithelial cells against H2O2-induced apoptosis through down-regulation of the alpha B-crystallin gene. J Biol Chem. 2001; 276:43435–43445. [PubMed: 11546795]

[39]. Mao YW, Liu JP, Xiang H, Li DW. Human alphaA- and alphaB-crystallins bind to Bax and Bcl-X(S) to sequester their translocation during staurosporine-induced apoptosis. Cell Death Differ. 2004; 11:512–526. [PubMed: 14752512]

[40]. Mikhailov V, Mikhailova M, Pulkrabek DJ, Dong Z, Venkatachalam MA, Saikumar P. Bcl 2 prevents Bax oligomerization in the mitochondrial outer membrane. J Biol Chem. 2001; 276:18361–18374. [PubMed: 11279112]

[41]. Rothbard JB, Kurnellas MP, Brownell S, Adams CM, Su L, Axtell RC, Chen R, Fathman CG, Robinson WH, Steinman L. Therapeutic effects of systemic administration of chaperone αB-crystallin associated with binding proinflammatory plasma proteins. J Biol Chem. 2012; 287:9708–9721. [PubMed: 22308023]

[42]. Li B, Li D, Li GG, Wang HW, Yu AX. P58(IPK) inhibition of endoplasmic reticulum stress in human retinal capillary endothelial cells in vitro. Mol Vis. 2008; 14:1122–1128. [PubMed: 18568130]

[43]. Koyama Y, Matsuzaki S, Gomi F, Yamada K, Katayama T, Sato K, Kumada T, Fukuda A, Matsuda S, Tano Y, Tohyama M. Induction of amyloid beta accumulation by ER calcium disruption and resultant upregulation of angiogenic factors in ARPE19 cells. Invest Ophthalmol Vis Sci. 2008; 49:2376–2383. [PubMed: 18515580]

[44]. Wang J, Lenardo MJ. Roles of caspases in apoptosis, development, and cytokine maturation revealed by homozygous gene deficiencies. J Cell Sci. 2000; 113:753–757. [PubMed: 10671365]

[45]. Dasmahapatra G, Lembersky D, Rahmani M, Kramer L, Friedberg J, Fisher RI, Dent P, Grant S. Bcl-2 antagonists interact synergistically with bortezomib in DLBCL cells in association with JNK activation and induction of ER stress. Cancer Biol Ther. 2009; 8:808–819. [PubMed: 19270531]

[46]. Gupta S, Cuffe L, Szegezdi E, Logue SE, Neary C, Healy S, Samali A. Mechanisms of ER Stress-Mediated Mitochondrial Membrane Permeabilization. Int J Cell Biol. 2010:170215. [PubMed: 20169117]

[47]. Zhang D, Lu C, Whiteman M, Chance B, Armstrong JS. The mitochondrial permeability transition regulates cytochrome c release for apoptosis during endoplasmic reticulum stress by remodeling the cristae junction. J Biol Chem. 2008; 283:3476–3486. [PubMed: 18056990]

[48]. Muyderman H, Wadey AL, Nilsson M, Sims NR. Mitochondrial glutathione protects against cell death induced by oxidative and nitrative stress in astrocytes. J Neurochem. 2007; 102:1369–1382. [PubMed: 17484727]

[49]. Kim HR, Lee GH, Cho EY, Chae SW, Ahn T, Chae HJ. Bax inhibitor 1 regulates ER-stress-induced ROS accumulation through the regulation of cytochrome P450 2E1. J Cell Sci. 2009; 122:1126–1133. [PubMed: 19339548]

[50]. Kozlov AV, Duvigneau JC, Miller I, Nurnberger S, Gesslbauer B, Kungl A, Ohlinger W, Hartl RT, Gille L, Staniek K, Gregor W, Haindl S, Redl H. Endotoxin causes functional endoplasmic reticulum failure, possibly mediated by mitochondria. Biochim Biophys Acta. 2009; 1792:521–530. [PubMed: 19327397]

[51]. Simon HU, Haj-Yehia A, Levi-Schaffer F. Role of reactive oxygen species (ROS) in apoptosis induction. Apoptosis. 2000; 5:415–418. [PubMed: 11256882]

[52]. Yaung J, Kannan R, Wawrousek EF, Spee C, Sreekumar PG, Hinton DR. Exacerbation of retinal degeneration in the absence of alpha crystallins in an in vivo model of chemically induced hypoxia. Exp Eye Res. 2008; 86:355–365. [PubMed: 18191123]

[53]. Kim YH, Choi MY, Kim YS, Han JM, Lee JH, Park CH, Kang SS, Choi WS, Cho GJ. Protein kinase C delta regulates anti-apoptotic alphaB-crystallin in the retina of type 2 diabetes. Neurobiol Dis. 2007; 28:293–303. [PubMed: 17904375]

[54]. Bousette N, Chugh S, Fong V, Isserlin R, Kim KH, Volchuk A, Backx PH, Liu P, Kislinger T, MacLennan DH, Emili A, Gramolini AO. Constitutively active calcineurin induces cardiac endoplasmic reticulum stress and protects against apoptosis that is mediated by alpha-crystallin-B. Proc Natl Acad Sci U S A. 2010; 107:18481–18486. [PubMed: 20937869]

[55]. Ruan Q, Han S, Jiang WG, Boulton ME, Chen ZJ, Law BK, Cai J. αB-Crystallin, an Effector of Unfolded Protein Response, Confers Anti-VEGF Resistance to Breast Cancer via Maintenance of Intracrine VEGF in Endothelial Cells. Mol Cancer Res. 2011; 9:1632–1643. [PubMed: 21984182]

[56]. Bhatt K, Feng L, Pabla N, Liu K, Smith S, Dong Z. Effects of targeted Bcl-2 expression in mitochondria or endoplasmic reticulum on renal tubular cell apoptosis. Am J Physiol Renal Physiol. 2008; 294:F499–507. [PubMed: 18160625]

[57]. Capano M, Crompton M. Biphasic translocation of Bax to mitochondria. Biochem J. 2002; 367:169–178. [PubMed: 12097139]

[58]. Fu HY, Okada K, Liao Y, Tsukamoto O, Isomura T, Asai M, Sawada T, Okuda K, Asano Y, Sanada S, Asanuma H, Asakura M, Takashima S, Komuro I, Kitakaze M, Minamino T. Ablation of C/EBP homologous protein attenuates endoplasmic reticulum-mediated apoptosis and cardiac dysfunction induced by pressure overload. Circulation. 2010; 122:361–369. [PubMed: 20625112]

[59]. Luetjens CM, Bui NT, Sengpiel B, Munstermann G, Poppe M, Krohn AJ, Bauerbach E, Krieglstein J, Prehn JH. Delayed mitochondrial dysfunction in excitotoxic neuron death: cytochrome c release and a secondary increase in superoxide production. J Neurosci. 2000; 20:5715–5723. [PubMed: 10908611]

[60]. Kadono T, Zhang XQ, Srinivasan S, Ishida H, Barry WH, Benjamin IJ. CRYAB and HSPB2 deficiency increases myocyte mitochondrial permeability transition and mitochondrial calcium uptake. J Mol Cell Cardiol. 2006; 40:783–789. [PubMed: 16678848]

[61]. Kamradt MC, Chen F, Cryns VL. The small heat shock protein alpha B-crystallin negatively regulates cytochrome c- and caspase-8-dependent activation of caspase-3 by inhibiting its autoproteolytic maturation. J Biol Chem. 2001; 276:16059–16063. [PubMed: 11274139]

[62]. Kamradt MC, Chen F, Sam S, Cryns VL. The small heat shock protein alpha B-crystallin negatively regulates apoptosis during myogenic differentiation by inhibiting caspase-3 activation. J Biol Chem. 2002; 277:38731–38736. [PubMed: 12140279]

[63]. Shin JH, Kim SW, Lim CM, Jeong JY, Piao CS, Lee JK. alphaB-crystallin suppresses oxidative stress-induced astrocyte apoptosis by inhibiting caspase-3 activation. Neurosci Res. 2009; 64:355–361. [PubMed: 19379782]

[64]. Carriere A, Carmona MC, Fernandez Y, Rigoulet M, Wenger RH, Penicaud L, Casteilla L. Mitochondrial reactive oxygen species control the transcription factor CHOP-10/GADD153 and adipocyte differentiation: a mechanism for hypoxia-dependent effect. J Biol Chem. 2004; 279:40462–40469. [PubMed: 15265861]

[65]. Kannan R, Sreekumar PG, Hinton DR. Novel roles for α-crystallins in retinal function and disease. Prog Ret Eye Res. 2012 in press.

- ER Stress in retinal pigment epithelium (RPE) leads to mitochondrial dysfunction
- ER stress in RPE results in apoptosis from activation of caspases -4 and -3
- ER stress mediated apoptosis in RPE involves PERK -eIf2α, ATF6 , and CHOP
- αB crystallin deficiency in RPE augment ER stress induced apoptosis
- αB crystallin overexpression protects RPE from ER stress induced apoptosis

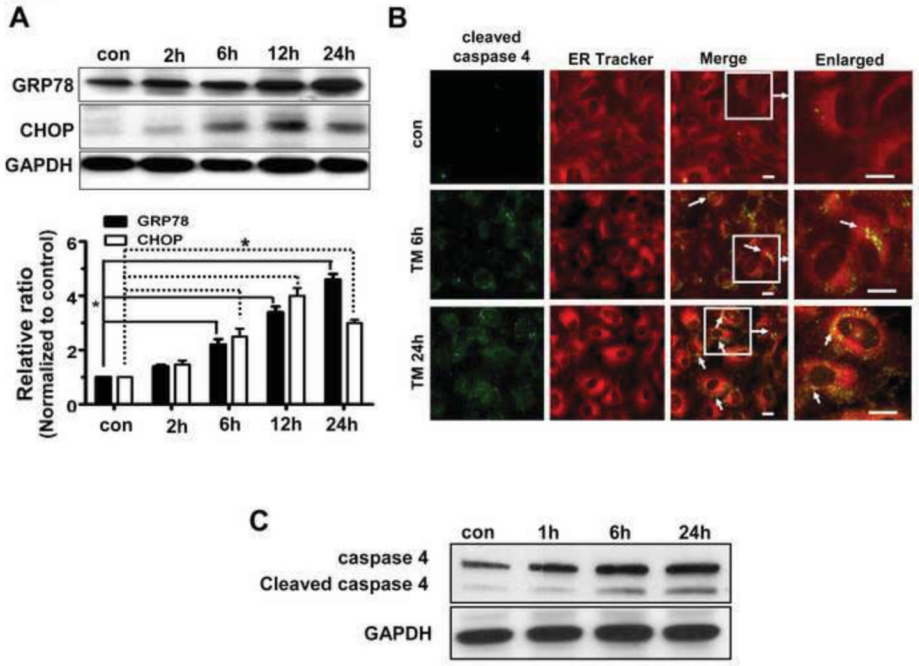

Fig.1. Induction of GRP78, CHOP and caspase 4 by TM treatment of hRPE cells

Confluent hRPE cells were treated with varying concentrations of TM for the duration shown. **A**. Expression of GRP78 and CHOP in hRPE cells treated with 3μg/ml TM by western blot analysis. Densitometric analysis showed a significantly increased expression of GRP78 and CHOP ($p<0.05$ vs controls) with increased time of treatment with TM. Values are the mean ± S.D. from three independent experiments. **B, C**. Effect of TM on cleaved caspase 4 expression by confocal microscopy (B) and immunoblot analysis (C). Activation of caspase 4 with increased duration of TM treatment is seen by western blot analysis which is confirmed by immunofluorescence of cleaved caspase 4 (green) and ER tracker (red). Double labeling is marked by white arrows. * $p<0.05$. Bar= 10 μm.

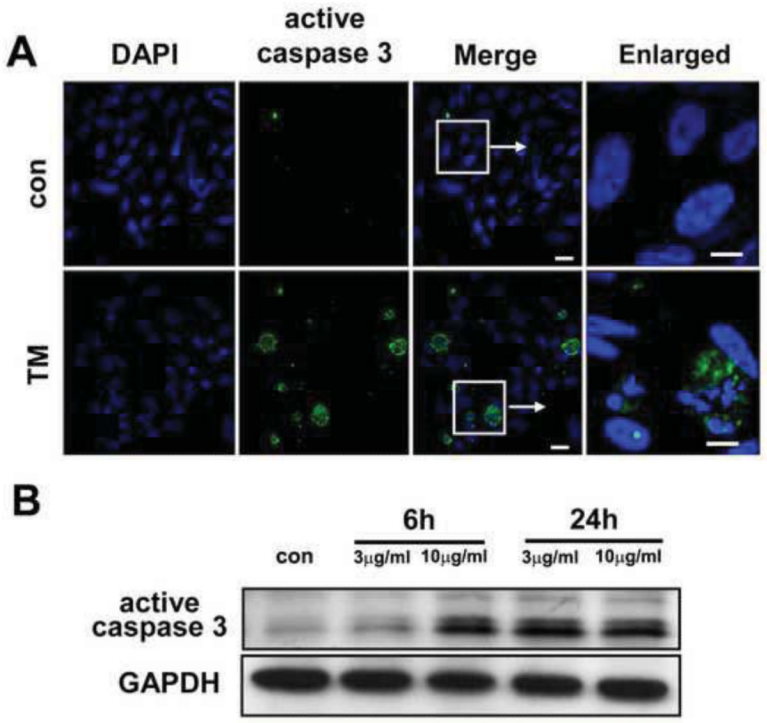

Fig.2. Activation of caspase 3 by TM-induced ER stress in hRPE cells

A. hRPE cells were treated with 3μg/ml or 10μg/ml TM for 6 h or 24 h. Immunostaining with active caspase 3 antibody showed the activation of caspase 3 (green) by confocal microscopy (A). DAPI (blue) was used to counterstain the nucleus. **B.** Western blot analysis of total cell lysates from hRPE cells treated with or without TM and probed with active caspase 3 antibody showed increased expression of active caspase 3 with 3 μg/ml for 24 h and 10 μg/ml for 6h TM treatments respectively. Bar= 10 μm for merged image and 5 μm for enlarged image.

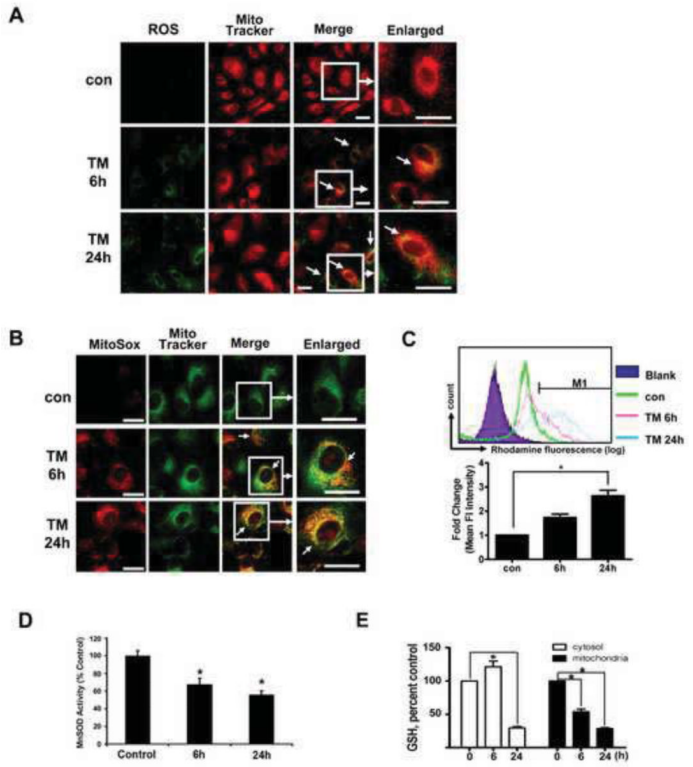

Fig.3. TM treatment of hRPE cells results in increased ROS in mitochondria, decreased MnSOD activity and depletion of mitochondrial GSH

A. hRPE cells were treated with 3 μg/ml TM for 6 h and 24 h. Carboxy-H2DCFDA and Mito Tracker were added to the cultures 60 min and 30 min before the end of the treatment respectively to achieve double labeling for ROS (green) and mitochondria (red). As seen in merged confocal images in A (white arrows), TM treatment caused marked production of ROS. The increased ROS mainly accumulated in mitochondria of RPE cells as shown by MitoSOX (red) and MitoTracker (green) as shown in B. **C.** Representative tracings from flow cytometric analysis demonstrating time dependent increase in mean fluorescent intensity of oxidized MitoSOX following 3μg/ml TM treatment (upper panel). The bar graphs (lower panel) show quantitation of time dependent changes in mean fluorescent intensity of oxidized MitoSOX following TM exposure. **D**. Effect of ER stress on MnSOD activity in RPE. SOD activity decreased significantly with 3μg/ml TM treatment at 6 h and 24 h. Data are expressed as % of control SOD values. **E.** Time dependent changes in reduced glutathione (GSH) levels in cytosolic and mitochondrial pools after exposure to 3 μg/ml TM showing progressive depletion of mitochondrial GSH with exposure time to TM. Data presented in the bar graphs are mean ± S.D. (n=3). * $p<0.05$. Bar: 10 μm.

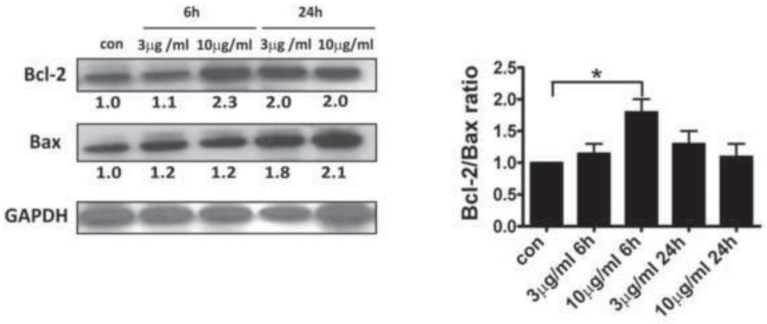

Fig.4. Up-regulation of Bcl-2 and Bax under ER stress

hRPE cells were cultured with or without TM (3 or 10 μg/ml) for 24h. Bcl-2 and Bax were analyzed on the same immunoblot of the whole cell lysates from TM treatment following stripping and reprobing. Normalization for Bcl-2 and Bax against GAPDH was made before calculating the Bcl-2/Bax ratio. The left panel shows a western blot from a representative experiment. The right panel shows the fold changes calculated by normalization of band density with GAPDH from three independent experiments. Values are mean ± S.D. * $p < 0.05$.

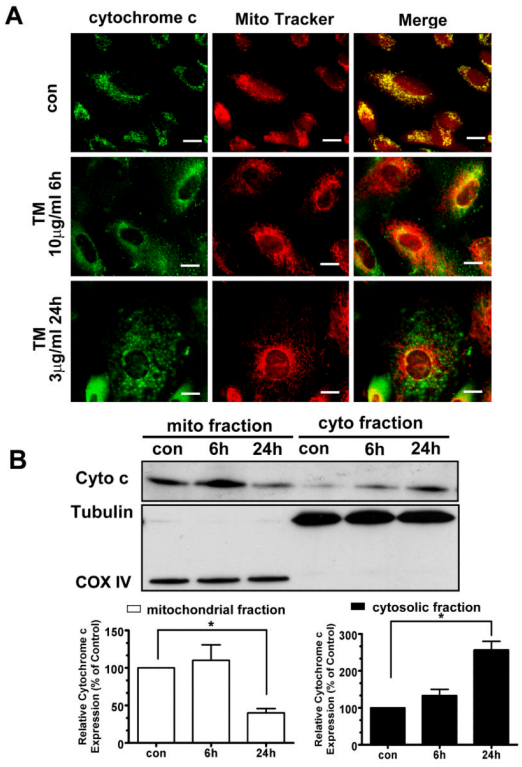

Fig.5. ER stress induces release of cytochrome c from hRPE mitochondria

A. hRPE cells treated with 3 μg/ml TM for 24 h and 10 μg/ml TM for 6 h were used for analysis of cytochrome c by immunofluorescence and western blot. The distribution of cytochrome c (green) and Mito Tracker (red) by confocal microscopy showed release of cytochrome c into cytosol under ER stress. **B.** Western blot analysis of cytochrome c in isolated mitochondrial and cytosolic fractions of hRPE cells exposed to 3 μg/ml TM for 24 h. The blot shows that especially after 24 h TM treatment, a significant amount of cytochrome c is released from mitochondria to cytosol (upper panel). The lower panels show the fold changes calculated by normalization of band density with anti-COX IV (mitochondrial protein marker) and anti-Tubulin (cytosolic protein marker), which further confirmed a >50% increase of cytochrome c in cytosol. Values are the mean±S.D.from three independent experiments. * $p< 0.05$. Bar: 10 μm.

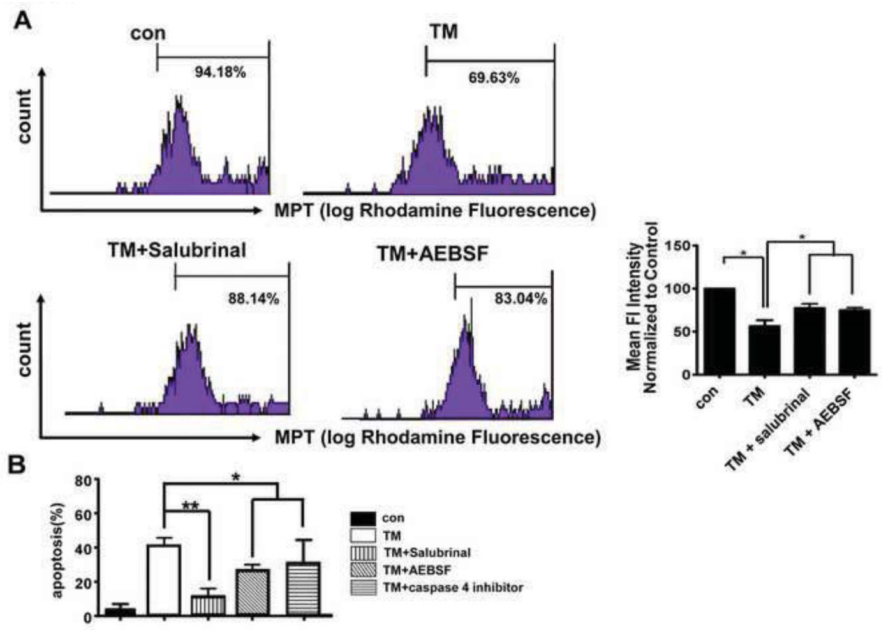

Fig.6. Effect of Salubrinal and AEBSF on increased mitochondrial permeability transition (MPT) and RPE cell death induced by TM

A. MPT was examined by flow cytometry of hRPE cells after indicated treatments. Quantitative analysis from three independent experiments. Flow cytometry experiments demonstrated that mean fluorescent intensity in mitochondria from TM-treated RPE decreased as compared to controls. Bar graph shows quantitation of fluorescent density from three independent experiments. Data presented are Mean ± S.D. *p<0.05. **B**. Quantitative analysis of the effect of salubrinal and AEBSF on apoptosis induced by 3 μg/ml TM by TUNEL assay. Pretreatment with 25 μM salubrinal, or 150 μM AEBSF, or 10μM caspase 4 inhibitor for 2 h significantly decreased the percent of apoptotic cells. *p<0.05. **p<0.01.

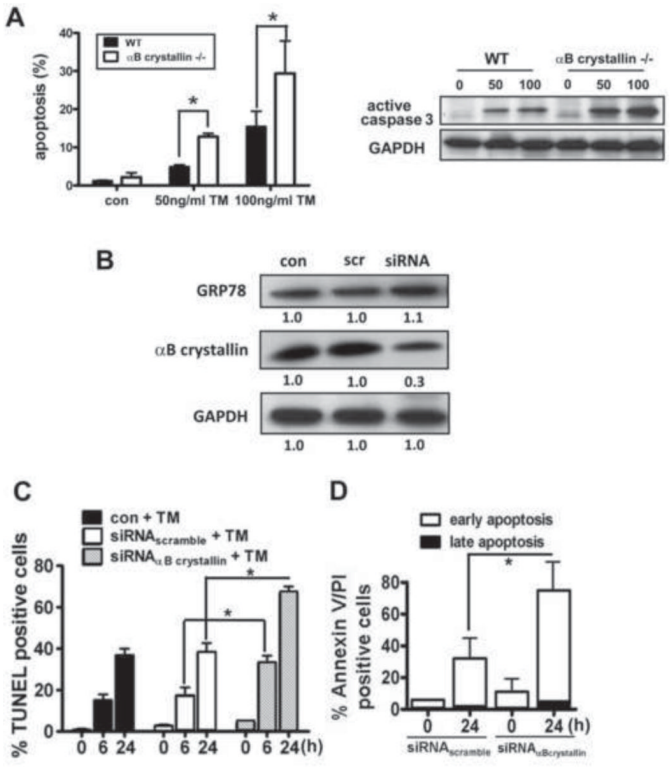

Fig.7. Deficiency of αB crystallin augments ER stress induced apoptosis

A. RPE cells from αB crystallin (−/−) mice grown to confluence were treated with 50ng/ml and 100ng/ml TM for 24 h and stained for apoptosis by TUNEL assay (left panel). Cell lysates from RPE cells of αB crystallin (−/−) mice and control mice were probed with active caspase 3 antibody (right panel). A dose dependent increase in apoptosis and active caspase was found which was significantly higher in αB crystallin (−/−) RPE vs control RPE. **B**. GRP78 and αB crystallin levels as determined by western blot analysis of αB crystallin siRNA transfected RPE showed a significant decrease in αB crystallin while GRP78 remained essentially unaltered. **C.** Quantitation of apoptotic cell death by confocal microscopy showing increased percentage of TUNEL positive cells in αB crystallin siRNA group. (D) In the αB crystallin siRNA transfected hRPE at the maximum ER stress used (3μg/ml TM for 24h), >90% of the dead cell population was AnnexinV+/PI indicating an apoptotic mechanism of cell death while <10% of cells were positive for both Annexin V and PI indicating either necrosis or later stage apoptosis. Values are mean ± S.D. from three independent experiments. *p<0.05.

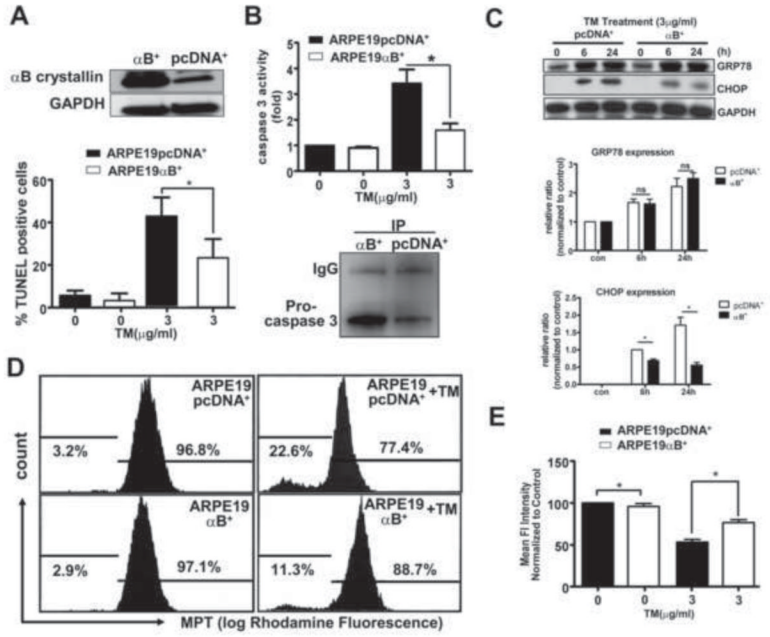

Fig.8. αB crystallin overexpression counteracts ER stress-induced apoptotic signaling cascades by inhibiting caspase 3 activity and CHOP and attenuates ER stress-induced mitochondrial defect

A. Western blots showing increased αB crystallin protein expression in the αB crystallin overexpressing ARPE-19 cells (ARPE19-B^+) as compared to transfection control cell line (ARPE19-$pcDNA^+$) (upper panel), The percentage of apoptotic cells after TM treatment by TUNEL assay was higher is in ARPE19-$pcDNA^+$ vs ARPE19-αB^+ group (lower panel). **B**. Caspase 3 activity in TM treated groups was higher than without TM and this activity in ARPE19-$pcDNA^+$ cells was found to be significantly higher ($p<0.05$) as compared to ARPE19-αB^+ cells (upper panel). Lower panel shows co Immunoprecipitation of αB crystallin and caspase 3 from stably transfected ARPE19-$pcDNA^+$ and ARPE19-αB^+ cells. **C.** Immunoblots showing the time course of CHOP expression in ARPE19-$pcDNA^+$ and ARPE19-α B^+cells, demonstrating overexpression of αB crystallin inhibits CHOP expression. **D.** Flow cytometric determination of MPT in ARPE19-$pcDNA^+$ and ARPE19-αB^+ cells treated with 3 μg/ml TM for 24 h. Flow cytometry experiments demonstrated more mean fluorescent intensity in mitochondria of ARPE19-αB^+ cells following 3 μg/ml TM treatment for 24 (left panel). Data shown in bar graphs are Mean ± S.D. (n=3). *$p<0.05$.

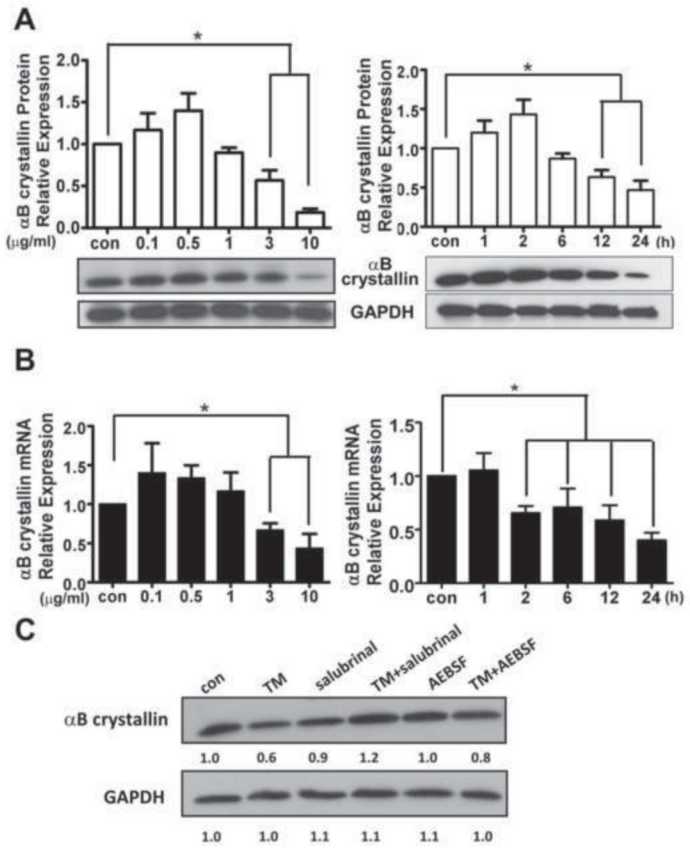

Fig.9. Tunicamycin-induced ER stress down-regulates expression of αB crystallin in hRPE cells

A. Time and dose dependency of αB crystallin protein expression in hRPE cells exposed to varying TM doses (0.1 – 10 μg/ml) for 24 h (left), and for varying durations (1 – 24 h) with 3μg/ml TM (right). In both time set and dose set conditions, the relative protein level of αB crystallin in control and treated cells were quantified and corrected using GAPDH as an internal control. Values are mean ± S.D from three independent experiments. **B**. Time and dose relationships of TM on αB crystallin mRNA measured by quantitative PCR from RPE cells. Transcriptional level of αB crystallin was expressed relative to internal GAPDH mRNA. Values are mean ± S.D from three independent experiments. C. Changes in αB crystallin protein expression in RPE cells under ER stress in the presence and absence of ER stress inhibitors. Cell lysates from RPE cells treated with TM in the presence or absence of Salubrinal (25 μM) and AEBSF (150 μM) for 24 h were analyzed by western blot analysis. *p<0.05 where indicated.